

Lanthanoid Coordination with a Tetrazole-Substituted Calix[4]diquinone and Calix[4]dihydroquinone

Lee Cameron,^a Aswin Rajagopalan,^a Laura Abad Galan,^a Rene Z.H. Phe,^a Brian W. Skelton,^b Massimiliano Massi,^a and Mark I. Ogden^{a,*}

^a Curtin Institute for Functional Molecules and Interfaces, School of Molecular and Life Science, Curtin University, GPO Box U 1987, Western Australia 6845

^b Chemistry M313, School of Biomedical, Biomolecular and Chemical Sciences, University of Western Australia, Crawley, Western Australia 6009

email: m.ogden@curtin.edu.au

url: <http://chemistry.curtin.edu.au>

Abstract

The tetrazole-functionalised calixdiquinone 5,17-di-*tert*-butyl-26,28-bis-(tetrazol-5-ylmethoxy)-calix[4]-25,27-diquinone **Q** was synthesised by chemical oxidation of the bis-tetrazole calix[4]arene precursor using PbO₂/HClO₄. The single crystal X-ray structure determination of **Q** confirmed the structure and showed binding of a water molecule in the solid state. Chemical reduction of **Q** to the dihydroquinone **QR** was achieved using N,N-diethylhydroxylamine. Comparison of the solution phase photophysical properties of **Q** or **QR** in the presence of terbium ions showed significant excitation only with **QR**, suggesting redox switching of the photophysical response may be possible with this or similar receptors.

Keywords: calixarene, lanthanide, quinone

Introduction

Calix[*n*]quinones are oxidised derivatives of calix[*n*]arenes where the phenol groups in the calix[*n*]arenes are oxidised to quinones. These macrocycles have attracted interest due to their capacity to act as ionophores, combined with useful electrochemical properties, and readily accessible further functionalisation.¹⁻¹¹ Calix[4]quinones have previously been synthesised from the oxidation of calix[4]arenes with thallium reagents, such as thallium trifluoroacetate.⁷ Thallium reagents are extremely toxic,¹² so there has been interest in developing alternative oxidation methodologies. For example, another synthetic pathway reported for the oxidation of calix[4]arenes uses aqueous ClO₂.¹³ This method, however, can only be applied to debutylated calix[4]arenes. An alternative method reported for the synthesis of calix[4]quinones from *p*-*t*-butylcalixarenes is oxidation with PbO₂/HClO₄, which has been reported to give similar yields to the thallium trifluoroacetate oxidation method.¹⁴ Calix[4]quinone synthesis has also been reported through electrochemical oxidation.¹ This method does not require chemical oxidising reagents, but can be more difficult to scale up.

Here, we have selected the PbO₂/HClO₄ oxidation to synthesise 5,17-di-*tert*-butyl-26,28-bis-(tetrazol-5-ylmethoxy)-calix[4]-25,27-diquinone **Q**. We also report the synthesis of the reduced analogue, 5,17-di-*tert*-butyl-11,23,25,27-tetrahydroxy-26,28-bis-(tetrazole-5-ylmethoxy)-calix[4]arene **QR** (Figure 1). The aim of the work was to compare the photophysical properties of lanthanoid complexes of these receptors, to determine if a redox-switchable light-emitting system could be developed.

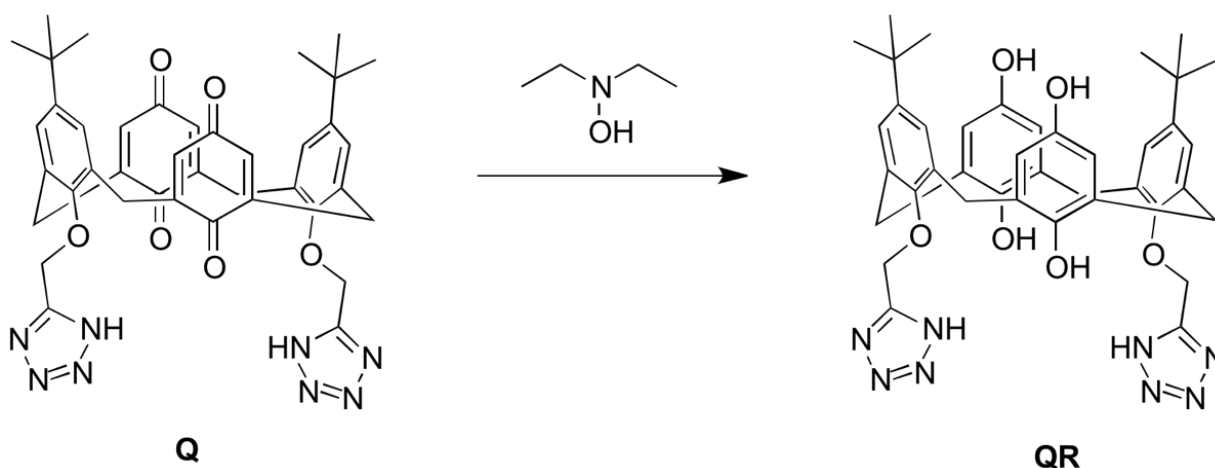


Figure 1. Structures of the targeted calixarene receptors.

Experimental

All chemical reagents and solvents were purchased from Sigma-Aldrich. The 5,11,17,23-tetra-*tert*-butyl-25,27-dihydroxy-26,28-ditetrazolylicalix[4]arene was synthesised following the literature method.¹⁵ Melting points were recorded on a VWR-IA9100 instrument using open ended capillaries. Infrared spectra (IR) were collected using FTIR-ATR, on a Perkin-Elmer Spectrum Two™ Infrared

Spectrometer. Nuclear Magnetic Resonance spectra were obtained using a Bruker Ultrashield 400TM instrument (400 MHz) at room temperature. Chemical shifts were recorded on the δ scale relative to the deuterated solvent (CD_3CN). High resolution mass spectrometry was performed using a Q Exactive™ Focus Hybrid Quadrupole-Orbitrap™ Mass Spectrometer from Thermo Fisher (Thermo Fisher Scientific Corporation, US).

Synthesis

5,17-Di-tert-butyl-26,28-bis-(tetrazole-5-ylmethoxy)-calix[4]-25,27-diquinone (Q)

The method was adapted from the literature.¹⁴ Lead oxide (0.346 g, 1.49 mmol), and perchloric acid (1 mL, 11.6 mmol) were added to a dichloromethane:acetone mixture (8 mL, 1:1) and stirred. A solution of 5,11,17,23-tetra-*tert*-butyl-25,27-dihydroxy-26,28-ditetrazolylcalix[4]arene (0.229 g, 0.282 mmol) in dichloromethane (2 mL), and acetone (2 mL) was slowly added dropwise to the lead solution. The mixture was stirred for 2 hours at room temperature, then filtered through celite, washing all the yellow solution through with dichloromethane (20 mL). Filtrate was washed with water (2 x 20 mL), collecting the organic phase which was dried over magnesium sulphate. Solvent was removed under reduced pressure, yielding yellow crystals. The crude product was sonicated in acetone (9 mL) for 15 minutes, before undergoing centrifugation (6500 rpm, 5 min) three times, replacing the supernatant acetone each time, before removing excess solvent, yielding bright yellow crystals. Yield: 50 mg (25 %) Crystal of appropriate quality for a single crystal structure determination were grown by slow evaporation of a methanol solution.

M.p.: Decomposes at 175 °C. ATR-FTIR (cm^{-1}): 3543.76 cm^{-1} (m, amine N-H), 2957.58 cm^{-1} (m, alkane C-H), 1658.58 cm^{-1} (s, ketone C=O), 1482.68 cm^{-1} (m, aromatic C=C), 1197.05 cm^{-1} (m, ether C-O). ¹H NMR (400 MHz, CD_3CN) δ 7.12 (s, 4H), 6.63 (s, 4H), 5.27 (s, 4H), 3.79 (d, $J = 14.2$ Hz, 4H), 3.34 (d, $J = 14.4$ Hz, 4H), 1.20 (s, 18H). ¹³C NMR (CD_3CN): δ (ppm) 207.48, 188.45, 187.23, 152.25, 149.26, 148.88, 133.58, 131.76, 128.47, 64.92, 35.04, 32.93, 31.54. HRMS (ESI/Q-TOF) m/z : $[\text{M} + \text{H}]^+$ Calcd for $\text{C}_{40}\text{H}_{41}\text{N}_8\text{O}_6$ 729.3144; Found 729.3135

5,17-Di-tert-butyl-11,23-dihydroxy-26,28-bis-(tetrazole-5-ylmethoxy)-calix[4]-25,27-dihydroxy (QR)

The reduction of the quinone was achieved following a modified literature procedure¹⁶ where a solution of *N,N*-diethylhydroxylamine (DEH) (2.4 mg, 0.027 mmol) was added into a solution of **Q** (20 mg, 0.027 mmol) in acetonitrile (7 mL) and stirred at room temperature for one hour. The resulting solution was neutralized with HCl (*ca.* 1M) and washed with water. The acetonitrile layer was then

dried under reduced pressure and the resulting product recrystallized from a mixture of acetonitrile/diethylether in 68% yield.

M.p.: 208 - 210 °C. ATR-FTIR (cm⁻¹): 3544.83 cm⁻¹ (m, amine N-H), 3035.68 (s, hydroxyl O-H), 2954.12 cm⁻¹ (m, alkane C-H), 1603.01 cm⁻¹ (m, hydroxyl C-O), 1463.84 cm⁻¹ (s, aromatic C=C), 1188.92 cm⁻¹ (s, ether C-O). ¹H NMR (400 MHz, CD₃CN) δ 7.22 (s, 4H), 6.56 (s, 4H), 5.49 (s, 4H), 4.14 (d, *J* = 12.8 Hz, 4H), 3.31 (d, 4H, *J* = 12.8 Hz, 4H), 1.21 (s, 18H). ¹³C NMR (CD₃CN): δ (ppm) δ 151.44, 151.15, 150.04, 145.14, 134.62, 130.87, 127.35, 115.81, 68.14, 35.08, 32.25, 31.46. HRMS (ESI/Q-TOF) *m/z*: [M + H]⁺ Calcd for C₄₀H₄₅N₈O₆: 733.3457. Found: 733.3448

Structure Determinations

The crystal data for **Q**·H₂O are summarised below. Crystallographic data for the structure were collected at 100(2) K on an Oxford Diffraction Gemini diffractometer using Cu Kα radiation. Following multi-scan absorption corrections and solution by direct methods, the structure was refined against *F*² with full-matrix least-squares using the program SHELXL-2014.¹⁷ Both *tert*-butyl groups were modelled as being disordered over two sets of sites with occupancies constrained to 0.5 after trial refinement. Geometries of the disordered atoms were also restrained to ideal values. Water molecule hydrogen atoms were included and refined with geometries restrained to ideal values. All remaining hydrogen atoms were added at calculated positions and refined by use of riding models with isotropic displacement parameters based on those of the parent atoms. Anisotropic displacement parameters were employed throughout for the non-hydrogen atoms.

Q·H₂O *M* = 746.81, yellow plate, 0.385 x 0.230 x 0.091 mm³, triclinic, space group *P* $\bar{1}$ (No. 2), *a* = 9.4048(3), *b* = 12.2576(4), *c* = 19.5606(6) Å, *α* = 81.938(3), *β* = 82.569(2), *γ* = 89.892(2)°, *V* = 2213.61(12) Å³, *Z* = 2, *D*_c = 1.120 g cm⁻³, *μ* = 0.645 mm⁻¹. *F*₀₀₀ = 788, 2*θ*_{max} = 67.32°, 44939 reflections collected, 7895 unique (*R*_{int} = 0.0417). Final *Goof* = 1.095, *R*₁ = 0.1036, *wR*₂ = 0.2477, *R* indices based on 6942 reflections with *I* > 2σ(*I*) (refinement on *F*²), |Δρ|_{max} = 0.512 e Å⁻³, 562 parameters, 15 restraints. CCDC 1894231

Supplementary material

Full details of the structure determinations for **Q** have been deposited with the Cambridge Crystallographic Data Centre as CCDC 1894231. These data can be obtained free of charge via <http://www.ccdc.cam.ac.uk/conts/retrieving.html>, or from the Cambridge Crystallographic Data Centre, 12 Union Road, Cambridge CB2 1EZ, UK; fax: (+44) 1223-336-033; or e-mail: deposit@ccdc.cam.ac.uk.

Results and Discussion

Ligand Synthesis and Characterization

The aim of this work was to develop an antenna ligand for lanthanoids that could be electrochemically switched on and off. Calixquinones were attractive electrochemically-active targets to achieve this, as they are readily synthesised, and have been studied as ionophores, for metal ions,⁴⁻⁷ and ion pairs.^{3, 8, 9} To develop the proof of principle, the aim here was to synthesise the oxidised and reduced forms of the ligand, which could then be complexed independently to the relevant lanthanoid cation. The bis-tetrazole substituted calix[4]arene was selected as a starting material, based on the previously reported use of this ligand as an antenna, where lanthanoid cations were found to be coordinated to the four phenol O atoms, and two tetrazole N atoms in the solid state.¹⁵ The synthesis of the oxidised bisquinone **Q** was achieved based on a literature method using lead oxide and perchloric acid that has been applied to other calixarenes.¹⁴ The only variation from the literature method was additional dilution of the lead oxide/perchloric acid mixture with the organic solvent, which in our hands gave higher yields and a cleaner product for this particular system.

In addition to the usual suite of characterisation techniques, crystals of appropriate quality for a single crystal x-ray structure determination were obtained by slow evaporation of a methanol solution. The results of the structure determination were consistent with the formulation **Q**·H₂O (Figure 2). The calixarene assumes a partial cone conformation. There are hydrogen bonds between the water molecule and the tetrazole rings and a quinone oxygen atom. There is also a hydrogen bond between the NH hydrogen and the other tetrazole group of the molecule related by a cell translation along the *b*-axis forming a 1-dimensional hydrogen bonded polymer. Hydrogen bonding geometrical details are listed in Table 1 with the hydrogen bonding polymer shown in Figure 3.

Table 1. Hydrogen bonds for **Q**·H₂O [Å and °].

D-H...A	d(D-H)	d(H...A)	d(D...A)	<(DHA)
N(112)-H(112)...N(312) ¹	0.88	1.94	2.778(5)	159.3
N(315)-H(315)...O(1)	0.88	1.92	2.785(5)	165.6
O(1)-H(1AO)...O(21)	0.826(19)	2.03(2)	2.834(4)	165(6)
O(1)-H(1BO)...N(115)	0.820(19)	2.04(3)	2.793(5)	152(6)

Symmetry transformations used to generate equivalent atoms: ¹ x,y+1,z

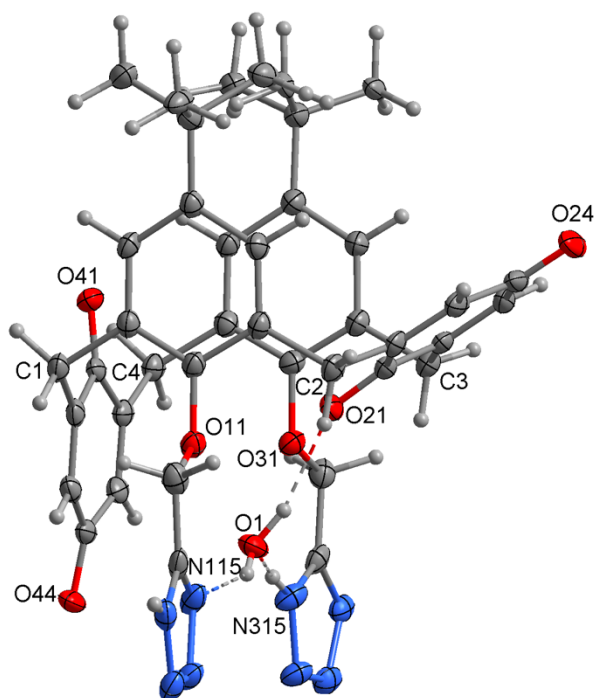


Figure 2 Structure of the molecule of $Q \cdot H_2O$. One set of the disordered atoms has been omitted.

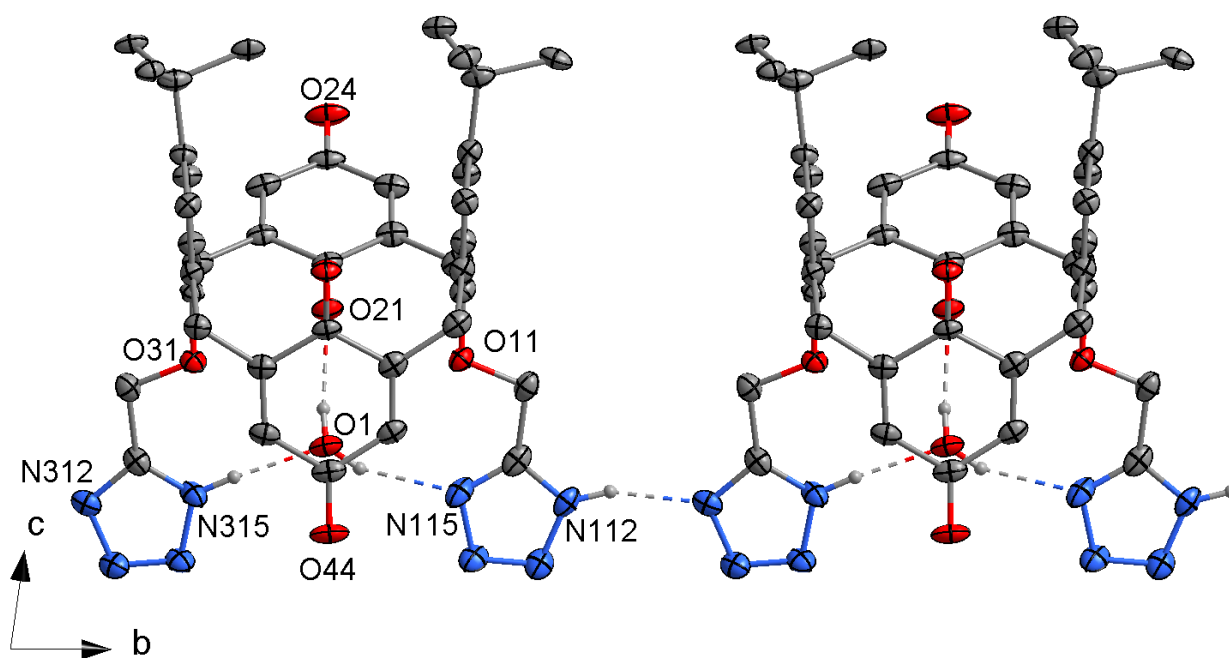


Figure 3 Structure of $Q \cdot H_2O$ projected along the a-axis showing the hydrogen bonded polymer. Hydrogen atoms not involved in the hydrogen bonding and one set of the disordered atoms have been omitted.

The chemical reduction of quinone calixarenes has been reported using aqueous sodium dithionite,¹⁸ and sodium borohydride.¹⁹ Here we chose to use N,N-diethylhydroxylamine (DEH), which has been reported to reduce quinones,¹⁶ to reduce Q to the dihydroquinone QR , to simplify the isolation of the product. Changes in the NMR spectra of the product, consistent with a reduction in conformational mobility due to additional hydrogen bonding, were observed, with peak widths reducing and the methylene AB doublet separation increasing from 0.45 to 0.83 ppm. HRMS confirmed that the target

had been isolated. With the ligands in hand, their complexation to lanthanoids was followed by studying their photophysical properties.

Absorbance studies:

The absorption of both ligands (**Q** and **QR**) were measured in ethanol with excess of triethylamine before and after the addition of excess of Gd^{3+} (Figure 4). Triethylamine was added to ensure the calixarene is deprotonated to maximise the stability of the lanthanoid-calixarene complex.¹⁵ The absorption profile of **Q** presents an intense band with maximum at 260 nm and a less intense but broader band in the 300-400 nm region. By comparison with the previously reported *p-t*-butylcalix[4]arene functionalized at the lower rim with two tetrazole moieties,¹⁵ the first band can be assigned to a $\pi-\pi^*$ transition centred on *tert*-butyl substituted phenyl rings and some contribution from $\pi-\pi^*$ of the tetrazole rings, while the extra broad band centered at 340 nm can be attributed to the $\pi-\pi^*$ of quinone rings. On the other hand, the absorption spectrum of the reduced ligand (**QR**) shows a blue shift of both bands appearing now below 250 nm and 300 nm, respectively. This blue shift may be caused by a more electron withdrawing effect coming from the phenolato ring in comparison to the quinone. When excess of the $GdCl_3 \cdot 6H_2O$ was added in the same solution a clear red shift characteristic of efficient coordination was found in the case of **QR**, while no significant shift was observed in the case of the **Q**. These data may suggest that coordination of the lanthanoid ions with ligand **Q** could be limited under the conditions tested.

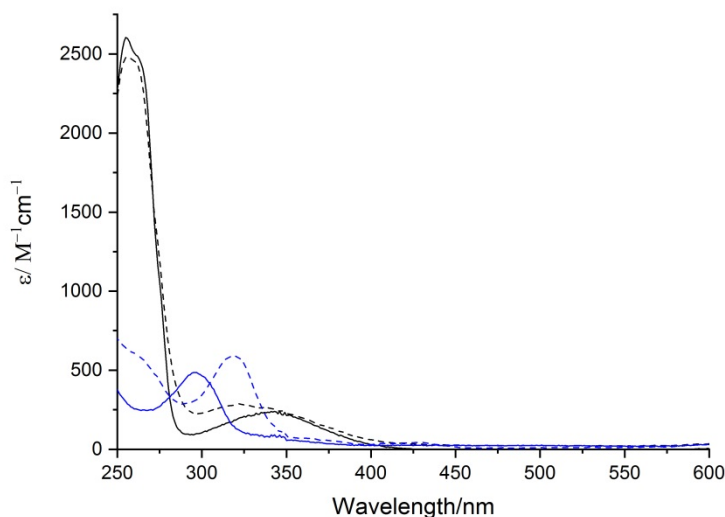


Figure 4. Absorption profiles of **Q** (black trace) and **QR** (blue trace) in ethanol with excess of triethylamine in the presence (dotted trace) and absence (full trace) of excess of $GdCl_3 \cdot 6H_2O$.

Photophysical Studies

In order to assess if ligands **Q** and **QR** can act as efficient antenna for the sensitisation of lanthanoids, the phosphorescent emission at 77K of the corresponding Gd^{3+} was studied. Unfortunately, the triplet state estimated from the 0-phonon transition, could only be assigned for **QR**. In this case, both singlet and triplet states were observed at $30,300\text{ cm}^{-1}$ and $27,030\text{ cm}^{-1}$, respectively (Figure 5). This triplet excited state energy should be high enough to sensitize the $^5\text{D}_4$ of Tb^{3+} ($\sim 20,400\text{ cm}^{-1}$).²⁰ In contrast the results for **Q** do not seem to present a clear triplet emission band, which may indicate again limited coordination of the metal ion (Figure S1).

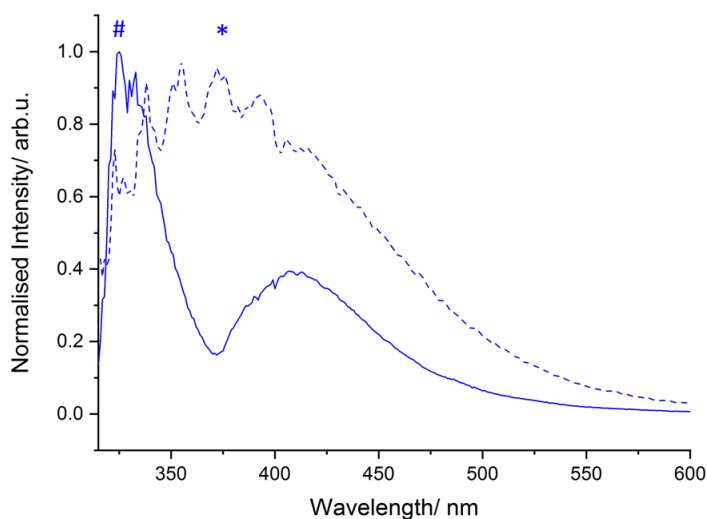


Figure 5. Emission ($\lambda_{\text{exc}}=300\text{ nm}$) of ligand **QR** (dark trace) and its Gd^{3+} complex (light trace) in ethanol at 77K. The # and * symbols indicates the 0-phonon transition of the singlet and triplet excited states, respectively.

Emission of both ligands were then studied in the presence of excess of Tb^{3+} in ethanol at room temperature. In the case of **Q**, no Tb^{3+} emission was observed and unexpectedly, only phosphorescence of the ligand could be seen (Figure S2). This could be explained by back energy transfer from the $^5\text{D}_4$ excited state of Tb^{3+} centered at $\sim 487\text{ nm}$, which lies relatively close to the apparent triplet state of **Q**, which was able to be assigned as $\sim 21,300\text{ cm}^{-1}$ based on these data. Therefore, while these results suggest that **Q** does coordinate to Tb^{3+} to a sufficient degree to undergo back transfer, it is confirmed as a poor antenna ligand at least for this lanthanoid cation.

In contrast, **QR** seems to sensitise more efficiently the $^5\text{D}_4$ of Tb^{3+} based on the presence of the line-like bands from the $^5\text{D}_4 \rightarrow ^7\text{F}_J$ ($J = 6, 5, 4, 3$) transition (Figure 6). The broad excitation spectrum found with emission wavelength at the main emission peak of Tb^{3+} (540 nm) suggests an efficient energy transfer whereas direct excitation of the Tb^{3+} excited states can be omitted. Indeed, when

compared with the excitation spectrum of the TbCl_3 employed for these studies a clear difference in shape of the excitation spectra can be observed. However, the baseline of the emission profile is not flat, which indicates possible emission of the ligand simultaneously occurring. The excited state lifetime (τ) found at 540 nm was fitted to a biexponential decay with $\tau = 134 \mu\text{s}$ (30%) + $42 \mu\text{s}$ (70%), which is consistent with emission from two different species.

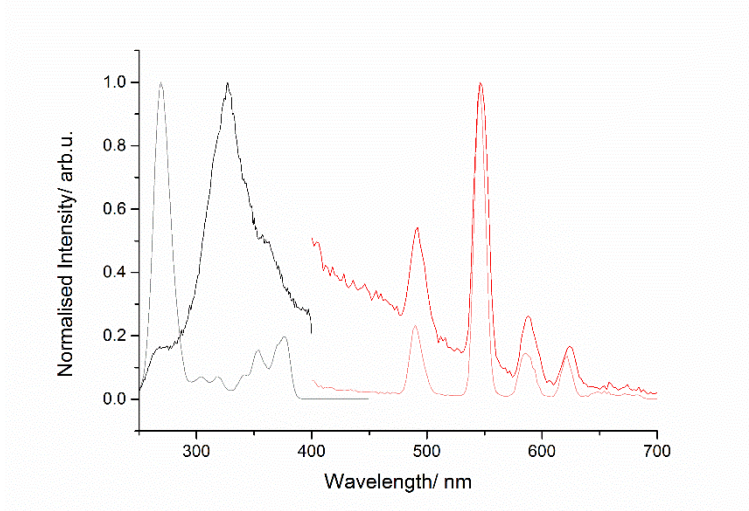


Figure 6. Normalised excitation ($\lambda_{\text{em}} = 540 \text{ nm}$) (black trace) and emission ($\lambda_{\text{exc}} = 300 \text{ nm}$) (red trace) plots for **QR** in the presence of excess of TbCl_3 (dark trace) and TbCl_3 (light trace) in EtOH (ca. 10^{-5}M).

Conclusions

The work presented here confirms that the photophysical response of a lanthanoid – calixquinone antenna assembly can be changed by reducing the molecule to the dihydroquinone analogue, where the response is a switching on of the lanthanoid emission in the case of terbium. Further work will be required to determine the relative influence of the change in the spectroscopic properties of the antenna, and the change in the binding efficacy of the ionophore.

Acknowledgements

We acknowledge the ECU Science Analytical Facility/ Thermo-Fisher Proof of Concept Laboratory for the HRMS measurements.

References

1. Vataj, R.; Louati, A.; Jeunesse, C.; Matt, D., *Electrochem. Commun.* **2000**, 2 (11), 769-775.

2. Leontiev, A. V.; Serpell, C. J.; White, N. G.; Beer, P. D., *Chem. Sci.* **2011**, *2* (5), 922-927.
3. Picot, S. C.; Mullaney, B. R.; Beer, P. D., *Chem. Eur. J.* **2012**, *18* (20), 6230-6237.
4. Webber, P. R. A.; Chen, G. Z.; Drew, M. G. B.; Beer, P. D., *Angew. Chem. Int. Edit.* **2001**, *40* (12), 2265-2268.
5. Webber, P. R. A.; Beer, P. D.; Chen, G. Z.; Felix, V.; Drew, M. G. B., *J. Am. Chem. Soc.* **2003**, *125* (19), 5774-5785.
6. Beer, P. D.; Gale, P. A.; Chen, Z.; Drew, M. G. B.; Heath, J. A.; Ogden, M. I.; Powell, H. R., *Inorg. Chem.* **1997**, *36* (25), 5880-5893.
7. Beer, P. D.; Chen, Z.; Gale, P. A.; Heath, J. A.; Knubley, R. J.; Ogden, M. I.; Drew, M. G. B., *J. Inclusion Phenom. Mol. Recognit. Chem.* **1994**, *19* (1), 343-359.
8. Lankshear, M. D.; Cowley, A. R.; Beer, P. D., *Chem. Commun.* **2006**, (6), 612-614.
9. Lankshear, M. D.; Dudley, I. M.; Chan, K. M.; Cowley, A. R.; Santos, S. M.; Fejix, V.; Beer, P. D., *Chem. Eur. J.* **2008**, *14* (7), 2248-2263.
10. Knighton, R. C.; Beer, P. D., *Chem. Commun.* **2014**, *50* (13), 1540-1542.
11. Kang, S. K.; Lee, O. S.; Chang, S. K.; Chung, D. S.; Kim, H.; Chung, T. D., *J Phys Chem C* **2009**, *113* (46), 19981-19985.
12. Huang, C.; Zhang, X.; Li, G.; Jiang, Y.; Wang, Q.; Tian, R., *Hum. Exp. Toxicol.* **2014**, *33* (5), 554-558.
13. Lin, Y.-L.; Yu, T.-S.; Wang, W.-Y.; Lin, L.-G., *Tetrahedron* **2006**, *62* (25), 6082-6089.
14. Lavendomme, R.; Troian-Gautier, L.; Zahim, S.; Reinaud, O.; Jabin, I., *Eur. J. Org. Chem.* **2016**, *2016* (9), 1665-1668.
15. D'Alessio, D.; Muzzioli, S.; Skelton, B. W.; Stagni, S.; Massi, M.; Ogden, M. I., *Dalton Trans.* **2012**, *41* (16), 4736-4739.
16. Fujita, S.; Sano, K., *J. Org. Chem.* **1979**, *44* (15), 2647-2651.
17. Sheldrick, G. M., *Acta Crystallogr. Sect. C: Struct. Chem.* **2015**, *71*, 3-8.
18. Genorio, B., *Acta Chim. Slov.* **2016**, *63* (3), 496-508.
19. Meddeb-Limem, S.; Malezieux, B.; Herson, P.; Besbes-Hentati, S.; Said, H.; Blais, J. C.; Bouvet, M., *J. Phys. Org. Chem.* **2005**, *18* (12), 1176-1182.
20. McCaw, C. S.; Murdoch, K. M.; Denning, R. G., *Mol. Phys.* **2003**, *101* (3), 427-438.

Lanthanoid Coordination with a Tetrazole-Substituted Calix[4]diquinone and Calix[4]dihydroquinone

Lee Cameron, Aswin Rajagopalan, Laura Abad Galan, Rene Z.H, Phe, Brian W. Skelton, Massimiliano Massi, and Mark I. Ogden

Supplementary Information

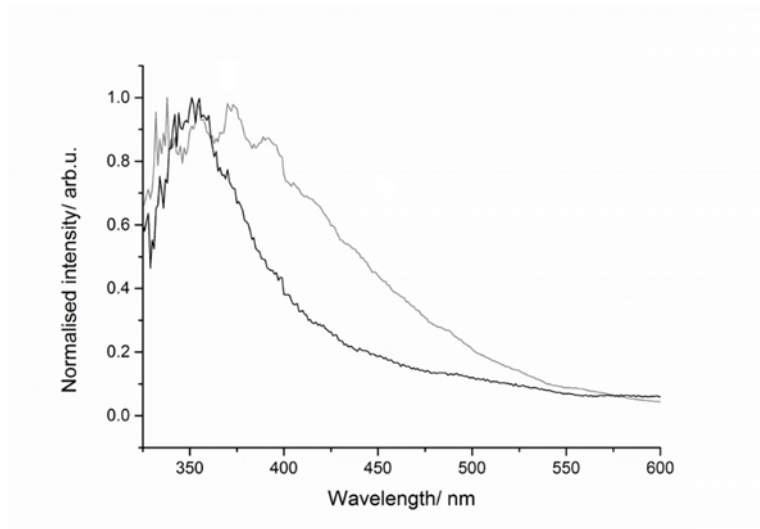


Figure S1. Normalised emission ($\lambda_{exc}=300$ nm) of ligand **Q** (dark trace) and its Gd³⁺ complex (light trace) in ethanol at 77K.

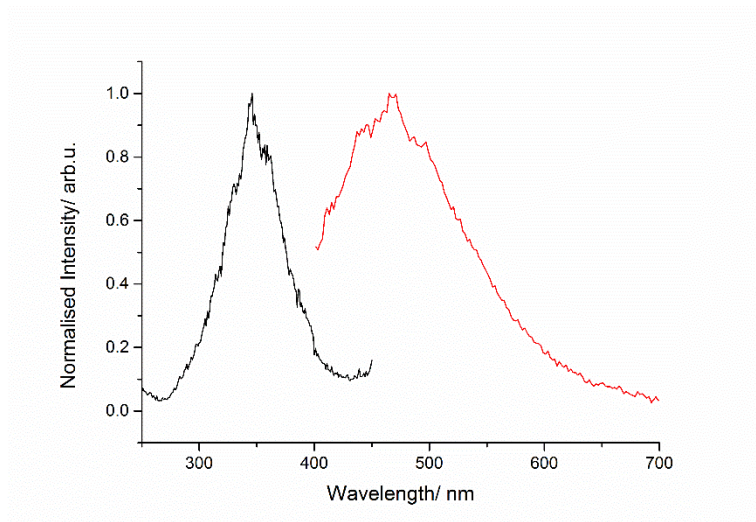


Figure S2. Normalised excitation ($\lambda_{em}=485$ nm) and emission ($\lambda_{exc}=300$ nm) plot for **Q** in the presence of excess of TbCl₃ in EtOH (ca. 10⁻⁵M).